Integral algorithm of exponential observables for interacting fermions in quantum Monte Carlo simulations

Xu Zhang [1], Gaopei Pan [1], Bin-Bin Chen,[1] Kai Sun,[2,*] and Zi Yang Meng [1,†]

[1]*Department of Physics and HKU-UCAS Joint Institute of Theoretical and Computational Physics, The University of Hong Kong, Pokfulam Road, Hong Kong SAR, China*

[2]*Department of Physics, University of Michigan, Ann Arbor, Michigan 48109, USA*

(Received 24 November 2023; revised 8 May 2024; accepted 9 May 2024; published 21 May 2024)

Exponential observables, formulated as $\ln\langle e^{\hat{X}}\rangle$ where $\hat{X}$ is an extensive quantity, play a critical role in the study of quantum many-body systems, examples of which include the free energy and entanglement entropy. Given that e^X becomes exponentially large (or small) in the thermodynamic limit, the accurate computation of the expectation value of this exponential quantity presents a significant challenge. In this paper, we propose a comprehensive algorithm to quantify these observables in interacting fermion systems, utilizing the determinant quantum Monte Carlo method. We have applied this algorithm to the two-dimensional square-lattice half-filled Hubbard model and π-flux t-V model. In the Hubbard model case at the strong-coupling limit, our method showcases a significant accuracy improvement on free energy compared to conventional methods that are derived from the internal energy, and in the t-V model, we indicate that the free energy offers a precise determination of the second-order phase transition. We also illustrate that this approach delivers highly efficient and precise measurements of the nth Rényi entanglement entropy. Even more noteworthy is that this improvement comes without incurring increases in computational complexity. This algorithm effectively suppresses exponential fluctuations and can be easily generalized to other models.

DOI: 10.1103/PhysRevB.109.205147

I. INTRODUCTION

Exponential observables such as the entanglement metrics and free energy hold a crucial role in unveiling the fundamental organizing principles of strongly correlated systems, as they offer full access to the partition function and universal conformal field theory (CFT) data of (quantum) many-body systems, which are otherwise hard to obtain. Such understandings have been extensively put forward in previous works [1–35]. Among these witnesses, entanglement entropy (EE) stands out as a vital metric for probing the behavior of interacting fermion systems in spatial dimension $D \geqslant 2$ [7–15,20,22–24]. In the case of free Fermi surfaces, the scaling form of EE is well established through the Widom-Sobolev formula, expressed as $L^{D-1}\ln L$, where L represents the linear system size [8–10]. However, for interacting fermion systems, the precise scaling form remains elusive and it is widely held that uncovering this scaling behavior could offer valuable insights into the fundamental CFT data associated with fermionic quantum critical points, low-energy collective modes, and topological information [5–12,20,24–26,31,36,37].

As another example of an exponential observable, the free energy is a key physics quantity that directly dictates the finite-temperature phase diagram of a many-body system [34,35]. For quantum Monte Carlo (QMC) simulations, the free energy also plays an important role in the sign problem, especially in sign bound theory [38–45]. Since the lower bound of the average sign amounts to a function of the free-energy difference between the original system and the reference system [40], calculating the free energy of the system helps one to understand how the average sign is affected by the free energy of the two systems, for example, to determine the relationship between the average sign and the phase transition [42–46].

However, the computation of EE and free energy in two-dimensional (2D) interacting fermion systems poses a formidable challenge. The computation hinges on accessing the observables exponentially proportional to L in the many-body partition functions, as detailed in prior studies [4,12–15,20,22–24]. To controllably compute these exponential observables within polynomial computational complexity, the determinant quantum Monte Carlo (DQMC) method has emerged as a promising solution [7,12,20,22,24,47,48]. Following Grover's pioneering work [7] where the many-body reduced density matrix is expanded according to the auxiliary field configuration subjected to the fermion Green's function, the algorithmic development of fermion EE has taken a long detour through the years.

Early attempts did not carry out the proper important sampling and therefore suffered from the poorly controlled data quality and less optimized computational complexity of $O(\beta N^4)$, where $\beta = 1/T$ is the inverse temperature and $N = L^D$ is the system size [12–15]. In Refs. [47,48], the integral idea has been proposed, while the computational complexity is still $O(\beta N^4)$. Recent developments, in particular the

*sunkai@umich.edu
†zymeng@hku.hk

incremental algorithm of EE computation [20], have managed to reduce the complexity to $O(\beta N^3)$ (the same as the general DQMC update), but add the extra procedure of sampling the entanglement area [22,24]. In Ref. [23], sampling of the entanglement area is replaced by incrementally raising the power of Grover's matrix, which makes the operation much easier (a similar development recently appeared in quantum spin systems [32]), and such polynomial form suppresses the exponential fluctuation of the observable. But no generic guidance appears on how often the entanglement area should be sampled or how small this polynomial power should be to suppress the exponential variance before actual computing. Therefore, the protocol still appears as *ad hoc*.

In this paper, we provide an elegant solution to this challenge of computing exponential observables combining the integral idea and the fast update routine. The integral idea [48] is that via simply introducing an auxiliary integral, measurement of exponential observables can be converted to a conventional observable without involving the expectation of any exponentially large (or small) quantities,

$$\ln\langle e^{\hat{X}}\rangle = \int_0^1 dt\,\langle \hat{X}\rangle_t. \tag{1}$$

Here, $\langle\cdot\rangle_t$ represents a modified average where the distribution probability is determined by an extra t with the factor of $e^{t\hat{X}}$. By applying this formula, all complications and challenges in measuring exponential observables have been fully eliminated, and the computational complexity becomes identical to the measurement of regular physics observables. Departing from this formula, we introduce a fast update integral algorithm in DQMC and use the 2D square-lattice half-filled Hubbard model and π-flux t-V model to illustrate the superior performance and reduced computational complexity of our algorithm. In the Hubbard model case, for free energy, the second and third Rényi EE are measured stably at finite temperature and their values at the low-temperature limit match well with the results from density matrix renormalization group (DMRG). In the t-V model case, our free-energy computation is precise for indicating the second-order phase transition.

We foresee that this method contributes to advancement in various directions, including discovering the unknown scaling form of EE for an interacting Fermi surface [27,36,37], the CFT information for various fermion deconfined quantum critical points (DQCPs), and symmetric mass generation (SMG), helping to identify fermion phase transitions beyond the Landau-Ginzburg-Wilson paradigm [28,31], indicating a first-order or second-order phase transition directly from free energy, computing domain-wall free energy in spin glass systems, [49,50], etc.

II. FORMULA FOR EXPONENTIAL OBSERVABLES

We review the formula for computing the second Rényi EE first, and then give a similar formula for computing the nth Rényi EE and free energy. The details of the fast update integral algorithm are given in the next section. From Ref. [7], we know the second Rényi EE $S_A^{(2)} \equiv -\ln[\mathrm{Tr}(\rho_A^2)]$ (here, A labels the set of sites whose degree of freedom is not traced in reduced density matrix ρ_A) can be expressed according to auxiliary field configuration $\{s_1, s_2\}$ as

$$S_A^{(2)} = -\ln\left(\frac{\sum_{s_1,s_2} P_{s_1}P_{s_2}\mathrm{Tr}\left(\rho_{A;s_1}\rho_{A;s_2}\right)}{\sum_{s_1,s_2} P_{s_1}P_{s_2}}\right), \tag{2}$$

where P_{s_i} is the importance sampling Monte Carlo weight for configuration s_i, $\rho_{A;s_i} = \det(G_{A;s_i})e^{c^\dagger \ln(G_{A;s_i}^{-1}-I)c}$ is the reduced density matrix, and $\mathrm{Tr}(\rho_{A;s_1}\rho_{A;s_2}) = \det[(I - G_{A;s_1})(I - G_{A;s_2}) + G_{A;s_1}G_{A;s_2}]$ is the determinant of the Grover matrix [7,20,22,23]. Here and below, we define the fermion Green's function as $G_{ij} \equiv \langle c_i c_j^\dagger\rangle$, where $\langle\cdot\rangle$ without the subscript always indicates the grand-canonical ensemble average which is used in the DQMC simulation. Since the EE is generally an extensive quantity dominated by the area law, a direct simulation by using $P_{s_1}P_{s_2}$ as the sampling weight and $\mathrm{Tr}(\rho_{A;s_1}\rho_{A;s_2})$ as the observable according to Eq. (2) will certainly give exponentially small values as $e^{-S_A^{(2)}} \sim e^{-al_A}$, where l_A is the boundary length of the entanglement region defined by the A set. This is why the direct simulation according to Eq. (2) is found to be unstable [12–15,22], i.e., one is sampling an exponentially small observable which can have exponentially large relative variances/fluctuations.

We notice Eq. (2) can be rewritten in an integral form,

$$\begin{aligned} S_A^{(2)} &= -\ln[f(1)] + \ln[f(0)] \\ &= -\int_0^1 dt\,\frac{\sum P_{s_1}P_{s_2}\mathrm{Tr}\left(\rho_{A;s_1}\rho_{A;s_2}\right)^t \ln\left[\mathrm{Tr}\left(\rho_{A;s_1}\rho_{A;s_2}\right)\right]}{\sum P_{s_1}P_{s_2}\mathrm{Tr}\left(\rho_{A;s_1}\rho_{A;s_2}\right)^t}, \end{aligned} \tag{3}$$

with $f(t) \equiv \sum P_{s_1}P_{s_2}\mathrm{Tr}(\rho_{A;s_1}\rho_{A;s_2})^t$ the entanglement partition function. Here and below, we omit auxiliary field labels in $\sum$ for notational simplicity. One can see that at each t, the original observable $\mathrm{Tr}(\rho_{A;s_1}\rho_{A;s_2})$ becomes logarithmic so that exponential fluctuations disappear naturally. In fact, one can choose other $f(t)$ satisfying a general integral formula,

$$S_A^{(2)} = -\int_0^1 dt\,\frac{\partial \ln[f(t)]}{\partial t}, \tag{4}$$

where the only requirements for $f(t)$ are $f(1) = \sum P_{s_1}P_{s_2} \times \mathrm{Tr}(\rho_{A;s_1}\rho_{A;s_2})$ and $f(0) = \sum P_{s_1}P_{s_2}$ [when taking $f(t) = \langle e^{t\hat{X}}\rangle$, we recover Eq. (1)].

Equation (3) can also be derived from taking the small polynomial power limit of the incremental algorithm [22–24] (see Appendix B for details). Besides the second Rényi EE, any exponentially small (or large) observable for interacting fermion systems in DQMC can be computed in a similar way. As examples, we introduce the formulas for the nth Rényi EE $S_A^{(n)}$,

$$\begin{aligned} S_A^{(n)} &\equiv -\frac{1}{n-1}\ln\left[\mathrm{Tr}\left(\rho_A^n\right)\right] \\ &= \frac{1}{1-n}\int_0^1 dt\,\frac{\sum P_s^n \mathrm{Tr}\left(\rho_{A;s}^n\right)^t \ln\left[\mathrm{Tr}\left(\rho_{A;s}^n\right)\right]}{\sum P_s^n \mathrm{Tr}\left(\rho_{A;s}^n\right)^t} \\ &\equiv \frac{1}{1-n}\left\langle \ln\left[\mathrm{Tr}\left(\rho_{A;s}^n\right)\right]\right\rangle_{s_1,s_2,\ldots,s_n;t}, \end{aligned} \tag{5}$$

and free energy F,

$$\begin{aligned} F &\equiv -\frac{1}{\beta}\ln(Z) \\ &= -\frac{1}{\beta}\int_0^1 dt \frac{\sum W_s P_s^t \ln(P_s)}{\sum W_s P_s^t} \\ &\equiv -\frac{1}{\beta}\langle \ln(P_s)\rangle_{s,t}. \end{aligned} \tag{6}$$

Here, $P_s^n \equiv \prod_{i=1}^n P_{s_i}$, $\rho_{A;s}^n \equiv \prod_{i=1}^n \rho_{A;s_i}$, W_s is the decouple coefficient independent of the Hamiltonian, and P_s is the determinant contribution from the Hamiltonian (e.g., if we decouple the Hubbard U term, such as $e^{\alpha\hat{O}^2} = \frac{1}{4}\sum_{l=\pm1,\pm2}\gamma(l)e^{\sqrt{\alpha}\eta(l)\hat{o}} + O(\alpha^4)$, where $\gamma(\pm1) = 1+\frac{\sqrt{6}}{3}$, $\gamma(\pm2) = 1-\frac{\sqrt{6}}{3}$, $\eta(\pm1) = \pm\sqrt{2(3-\sqrt{6})}$, and $\eta(\pm2) = \pm\sqrt{2(3+\sqrt{6})}$, then the part of $\frac{\gamma(l)}{4}$ is the W_s term and, after tracing out the fermion degree of freedom, the determinant part is the P_s term [51]).

III. DQMC INTEGRAL ALGORITHM

Next we describe how to implement our integral algorithm in the DQMC simulation. To compute the nth Rényi EE, one still needs a generic fast update scheme to guarantee the overall $O(\beta N^3)$ computational complexity [20]. First, let us review the fast update formulas for Green's functions $G \to G'$,

$$\begin{aligned} G'(\tau,\tau) &\equiv G(\tau,\tau) - \frac{1}{R_0}G(\tau,\tau)\Delta(i,\tau)[I - G(\tau,\tau)], \\ G'(\tau,0) &\equiv G(\tau,0) + \frac{1}{R_0}G(\tau,\tau)\Delta(i,\tau)G(\tau,0), \\ G'(0,\tau) &\equiv G(0,\tau) - \frac{1}{R_0}G(0,\tau)\Delta(i,\tau)[I - G(\tau,\tau)], \\ G'(0,0) &\equiv G(0,0) + \frac{1}{R_0}G(0,\tau)\Delta(i,\tau)G(\tau,0), \end{aligned}$$

where $R_0 \equiv \frac{\det\{I + B(\beta,\tau)[I+\Delta(i,\tau)]B(\tau,0)\}}{\det[I+B(\beta,0)]} = 1 + \Delta_{i,i}(i,\tau)[I - G(\tau,\tau)]_{i,i}$. (7)

Here we define $\Delta(i,\tau) = e^{V[s'(i,\tau)]}e^{-V[s(i,\tau)]} - I$ to update auxiliary field $s(i,\tau)$ and $B(\tau,\tau') = \prod_{\nu=\tau}^{\tau'} e^{H_s(\nu)}$ to represent the product of the decoupled partition function from imaginary time slices $\tau, \tau-1, \ldots, \tau'$. In comparison, the nth Grover matrix can be written as

$$g_{A;s_1,s_2,\ldots,s_n} \equiv \prod_i \left(G_{A;s_i}\right)\left[I + \prod_j \left(G_{A;s_j}^{-1} - I\right)\right]. \tag{8}$$

To simplify the notation, we further ignore the imaginary-time label for Green's function $G(0,0)$ at zero imaginary time, where reduced density matrices are defined accordingly. It is easy to generalize to a zero-temperature version, where we just need to replace $G(\tau,0), G(0,\tau), G(0,0)$ with $G(\tau,\theta), G(\theta,\tau), G(\theta,\theta)$, where θ is the projection length towards the ground state and all the formulas and conclusions still hold [24]. Update within s_j will not affect $G_{A;s_i}$ for any $i \neq j$. Assuming we want to update within s_1, we define an auxiliary matrix,

$$\begin{aligned} C_{A;s_1} &\equiv G_{A;s_1}\left[I + \prod_j \left(G_{A;s_j}^{-1} - I\right)\right] \\ &= I + G_{A;s_1}\left[I - \prod_{j>1}\left(G_{A;s_j}^{-1} - I\right)\right] \\ &\equiv I + G_{A;s_1}M_{A;s_1}, \end{aligned} \tag{9}$$

where $M_{A;s_1} \equiv I - \prod_{j>1}(G_{A;s_j}^{-1} - I)$ for notational convenience and remember $G_{A;s_1'} = G_{A;s_1} + G_{A;s_1}(0,\tau)\Delta(i,\tau)G_{A;s_1}(\tau,0)/R_0$. One will see that $C_{A;s_1}$ serves as the Grover matrix in Ref. [20] and has a better stability when n is increasing. We then use the Sherman-Morrison formula to compute the updated $C_{A;s_1'}^{-1}$ and determinant ratio between two nth Grover matrices,

$$\begin{aligned} C_{A;s_1'}^{-1} &= C_{A;s_1}^{-1}\left(I + \frac{G_{A;s_1}(0,\tau)\Delta(i,\tau)G_{A;s_1}(\tau,0)M_{A;s_1}C_{A;s_1}^{-1}}{R_0R_n}\right), \\ R_n &\equiv \frac{\det\left(g_{A;s_1',s_2,\ldots,s_n}\right)}{\det\left(g_{A;s_1,s_2,\ldots,s_n}\right)} = \frac{\det(C_{A;s_1}^{-1})}{\det(C_{A;s_1'}^{-1})} \\ &= 1 - \frac{1}{R_0}\Delta_{i,i}(i,\tau)G_{i,A;s_1}(\tau,0)M_{A;s_1}\left(C_{A;s_1}\right)^{-1}G_{A,i;s_1}(0,\tau). \end{aligned} \tag{10}$$

In this formula, $R_0, G_{A;s_1}(\tau,0), G_{A;s_1}(0,\tau), \Delta(i,\tau)$ come from the Green's function update routine and $M_{A;s_1}$ remains the same when updating s_1, so that computing $R_n, C_{A;s_1'}^{-1}$ from $C_{A;s_1}^{-1}$ has the same complexity $[O(N^2)]$ as the updating Green's function. In addition, one also needs formulas to update s_i other than the $i=1$ case and carry on numerical stabilization. Similar to the $B(\tau,\tau')$ matrix, we define $D(i,j) \equiv \prod_{k=i}^j (G_{A;s_k}^{-1} - I)$. Then we can write $C_{A;s_i}^{-1}$ and $M_{A;s_i}$ in a simple form,

$$\begin{aligned} C_{A;s_i}^{-1} &= [I + D(i,n)D(1,i-1)]^{-1}G_{A;s_i}^{-1}, \\ M_{A;s_i} &= I - D(i+1,n)D(1,i-1). \end{aligned} \tag{11}$$

One can check that the determinant of $C_{A;s_i}\prod_{j\neq i}(G_{A;s_j})$ is the same as $g_{A;s_1,s_2,\ldots,s_n}$. And we use the formula above to carry on numerical stabilization. To stably derive the logarithm

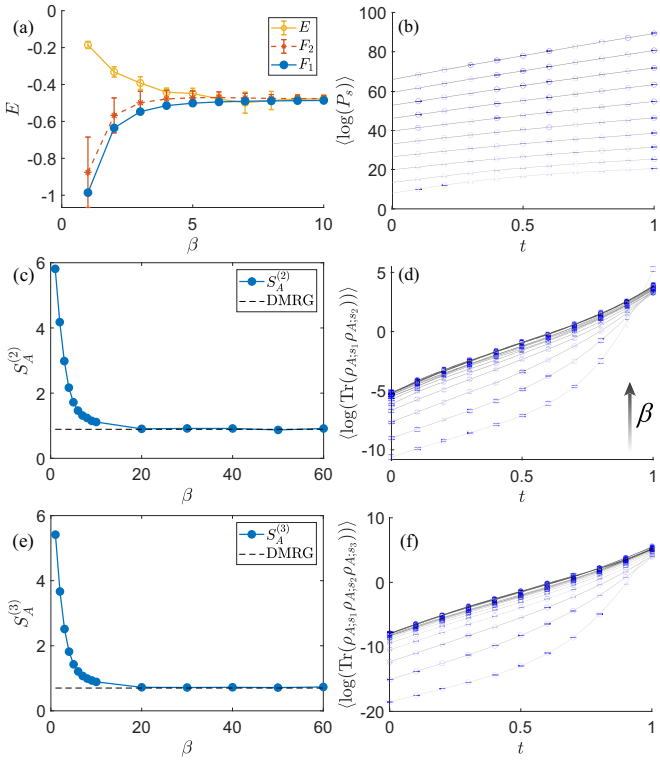

FIG. 1. (a) Internal energy density E, free-energy density F_2 derived by solving $E(\beta) = -\frac{\partial[\ln(Z)]}{\partial\beta} = \frac{\partial(\beta F_2)}{\partial\beta}$, and free-energy density F_1 according to Eq. (6). (b),(d),(f) $\langle\ln(P_s)\rangle$, $\langle\ln[\mathrm{Tr}(\rho_{A;s_1}\rho_{A;s_2})]\rangle$ and $\langle\ln[\mathrm{Tr}(\rho_{A;s_1}\rho_{A;s_2}\rho_{A;s_3})]\rangle$ for different β points used in (a),(c),(e) from small to large, corresponding to circles from bottom to top. Black lines show the fitting where the small slopes indicate a small fluctuation for $\langle\ln(P_s)\rangle$ at each t point. (c) The second EE $S_A^{(2)}$ converging with β to 0.89, which is consistent with DMRG at zero temperature. (e) The third EE $S_A^{(2)}$ converging with β to 0.7, which is consistent with DMRG at zero temperature.

determinant of the nth Grover matrix, one should separate the singular-value matrix, trace the logarithm of it, and add the logarithm determinant of other matrices.

IV. APPLICATION TO FERMION HUBBARD MODEL

In this section, we present the simulation results of free energy, the second and third Rényi EE for a 2D square-lattice fermion Hubbard model at half filling,

$$H = -t\sum_{\langle ij\rangle;s} c^\dagger_{i;s}c_{j;s} + U\sum_i (n_{i;\uparrow} + n_{i;\downarrow} - 1)^2. \tag{12}$$

A few implementational considerations and the proof of absence of the sign problem are listed in Appendix C; here we only focus on the results. In Figs. 1(a) and 1(b), we show the results for free energy for $L = 4, U/t = 8, \beta \in [1, 10]$ with cylinder geometry. One can see that free energy F_1 derived from Eq. (6) has a smaller fluctuation than internal energy. And free energy F_2 derived from integrating internal energy data according to $E(\beta) = -\frac{\partial[\ln(Z)]}{\partial\beta} = \frac{\partial(\beta F_2)}{\partial\beta}$ even has a much larger error bar coming from E.

In Figs. 1(c) and 1(d), we show the results of the second Rényi EE at the same parameter setting with entanglement

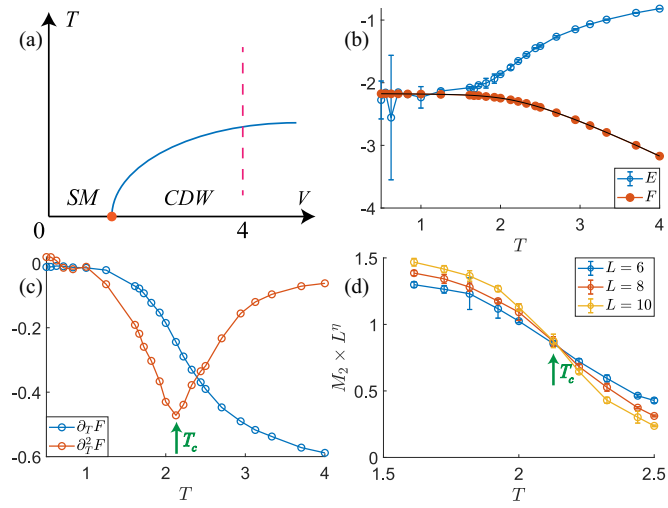

FIG. 2. (a) Schematic phase diagram of a spinless fermion π-flux half-filled square-lattice t-V model. The orange point indicates a $N = 2$ chiral-Ising transition in (2++1)D separating Dirac semimetal (SM) and charge density wave (CDW) phases. The blue line indicates a 2D Ising transition and our simulation goes along the dashed red line at $V = 4$ where a finite-temperature phase transition occurs. (b) Directly measured internal energy density E and free-energy density F measured by integral algorithm vs temperature T for system size $L \times 2L$ with $L = 6$ ($L = 8, 10$ have a similar internal energy and free-energy density). (c) First-order ($\partial_T F$) and second-order ($\partial_T^2 F$) derivative of free energy for system size $L = 6$, where the sharp dip at the green arrow at $T_c \approx 2.1$ in $\partial_T^2 F$ indicates the second-order phase transition temperature. (d) Finite-temperature phase transition shown by the green arrow at $T_c \approx 2.1$ determined by 2D Ising finite-size scaling [$M_2 \equiv \sum_{i,j}\frac{\alpha_i\alpha_j}{L^4}\langle(n_i - \frac{1}{2})(n_j - \frac{1}{2})\rangle$, where $\alpha_i = \pm 1$ for $i \in A, B$ sublattice and $\eta = \frac{1}{4}$ for 2D Ising university class].

area of $L \times L/2$ bipartitioning a cylinder geometry to compare with the DMRG result at zero temperature. The third Rényi EE with the same parameter and the comparison with DMRG are shown in Figs. 1(e) and 1(f). Our results show a very small sampling error for both free energy and EE. The low-temperature limit also matches well with DMRG.

V. APPLICATION TO t-V MODEL

In this section, we present the simulation results of free energy for a 2D square-lattice spinless fermion π-flux t-V model at half filling,

$$H = -\sum_{\langle ij\rangle} te^{i\phi_{ij}}c^\dagger_i c_j + V\sum_{\langle ij\rangle}\left(n_i - \frac{1}{2}\right)\left(n_j - \frac{1}{2}\right). \tag{13}$$

Here we set $t = 1$ and take the gauge choice $e^{i\phi_{ij}} = 1$ for the x-direction ij bonds and $e^{i\phi_{ij}} = \pm 1$ for even (odd) column y-direction ij bonds. The sign problem is proved to be free [52–54] and the ground-state transition from the Dirac semimetal to the charge density wave (CDW) insulator is found to belong to the Gross-Neveu chiral-Ising universality [55,56]. We focus on the large V ($V = 4$) case to detect the finite-temperature 2D Ising phase transition from the disorder phase to the CDW phase from free energy. The result is shown in Fig. 2. One can see that the free-energy measurement is

even better than the internal energy, as shown in Fig. 2(b), and the phase transition point indicated by the second-order derivative of the free energy for a single size [Fig. 2(c)] matches well with the canonical finite-size scaling result, as shown in Fig. 2(d).

VI. DISCUSSIONS

In this paper, we develop a fast update integral algorithm in DQMC, which converts measurements of exponential observables into conventional observables. This offers an elegant solution to the challenging problem of calculating exponential observables by fully suppressing the exponential fluctuations. Considering the current strong interest in entanglement entropy and determining the rich phase diagram of strongly correlated spin/electronic systems, this highly efficient approach of computing Rényi entropy and free energy has potentially broad applications to a wide range of physical systems. In our illustration of the 2D Hubbard model, the computed free energy has a smaller error than the internal energy at large Hubbard U. In the example of the t-V model, the derivative of free energy offers precise determinations of the phase transition. For systems with sophisticated interaction, such as twisted bilayer graphene and quantum Moiré systems [57–60], our approach also offers a much simpler way to access the free energy only from the Green's function without invoking the Wick decomposition for the four fermion interactions. In addition, our method offers generic and easy access to the nth Rényi EE, negativity [61,62], and entanglement spectrum [63,64] without incurring increases in computational complexity. Finally, our algorithm can also be generalized directly to the zero-temperature version projector QMC.

ACKNOWLEDGMENTS

X.Z. thanks G. Han for inspiring information theory lectures. We thank Y. D. Liao for discussion on the integral algorithm. We are thankful for the support from the Research Grants Council (RGC) of Hong Kong Special Administrative Region (SAR) of China (Projects No. 17301721, No. AoE/P701/20, No. 17309822, No. C7037-22GF, No. 17302223), the ANR/RGC Joint Research Scheme sponsored by the RGC of Hong Kong SAR of China and French National Research Agency (Project No. A_HKU703/22), and the HKU Seed Funding for Strategic Interdisciplinary Research. We are thankful for the HPC2021 system under the Information Technology Services, University of Hong Kong, and the Beijng PARATERA Tech CO. Ltd. [65] for providing HPC resources that have contributed to the research results reported within this paper.

APPENDIX A: IMPLEMENTATIONAL CONSIDERATIONS FOR THE INTEGRAL ALGORITHM

We list a few technical considerations when performing a practical calculation. The first one is that when we discretize the integral over t naively (e.g., use $-\frac{1}{N_k}\sum_{i=1}^{N_k}\langle \ln[\mathrm{Tr}(\rho_{A;s_1}\rho_{A;s_2})]\rangle_i$ to compute the 2nd Rényi entropy), the results must be larger than their true values. This indicates that the function $\frac{\partial \ln[f(t)]}{\partial t} = \langle \ln[\mathrm{Tr}(\rho_{A;s_1}\rho_{A;s_2})]\rangle_t$ is an increasing function. We notice the second-order derivative $\frac{\partial^2 \ln[f(t)]}{\partial t^2} = \langle \ln[\mathrm{Tr}(\rho_{A;s_1}\rho_{A;s_2})]^2\rangle_t - \langle \ln[\mathrm{Tr}(\rho_{A;s_1}\rho_{A;s_2})]\rangle_t^2 \geqslant 0$ indicates the fluctuation for $\langle \ln[\mathrm{Tr}(\rho_{A;s_1}\rho_{A;s_2})]\rangle_t$. As long as the slope is not sharp (i.e., indicating mild fluctuation), we can compute $\langle \ln[\mathrm{Tr}(\rho_{A;s_1}\rho_{A;s_2})]\rangle_t$ accurately at a given sequence of t points and numerically integrate within [0,1] to derive the second Rényi entropy. The corresponding results are shown in Figs. 1(c) and 1(d).

The second point is that one may observe that the sampling may not be "importance sampling" for a small t when computing the free energy. One can check the formula for free energy at $t \to 0$ limit, where the weight becomes independent with determinant P_s as well as the Hamiltonian so that one actually updates the auxiliary fields randomly. This can also be seen with the increasing acceptance ratio as $t \to 0$. One way to avoid this inefficient sampling is to update by the propose-accept/reject method for small t. Assuming $n \approx 1/t$, we can propose n auxiliary fields update and then determine whether or not to accept. This will recover the normal acceptance ratio as $t = 1$.

The third point is about the computation of $\ln[\mathrm{Tr}(\rho_{A;s_1}\rho_{A;s_2})]$ or $\ln(P_s)$ for each configuration. Directly computing the determinant will derive an exponentially small (or large) number and the exponent is hard to compute accurately using the logarithm. A more efficient way is to utilize the numerical stabilization step for computing, say, logarithm determinant of the Green's function,

$$\begin{aligned} G(\tau,\tau) &\equiv [I + B(\tau,0)B(\beta,\tau)]^{-1} \\ &\equiv (I + U_R D_R^{>} D_R^{<} V_R V_L D_L^{<} D_L^{>} U_L)^{-1} \\ &= U_L^{-1}(D_L^{>})^{-1}[(D_R^{>})^{-1}(U_L U_R)^{-1}(D_L^{>})^{-1} + D_R^{<} V_R V_L D_L^{<}]^{-1}(D_R^{>})^{-1} U_R^{-1}, \\ \ln\{\det[G(\tau,\tau)]\} &= -\ln\{\det[(D_R^{>})^{-1}(U_L U_R)^{-1}(D_L^{>})^{-1} + D_R^{<} V_R V_L D_L^{<}]\} \\ &\quad - \ln[\det(U_L)] - \ln[\det(U_R)] - \mathrm{Tr}[\ln(D_L^{>})] - \mathrm{Tr}[\ln(D_R^{>})]. \end{aligned} \tag{A1}$$

Here, for diagonal positive matrix D, we decompose it according to the diagonal element larger ($D^{>}$) or smaller ($D^{<}$) than 1, i.e., $D \equiv D^{>}D^{<}$. In this way, one can compute $\ln\{\det[G(\tau,\tau)]\}$ stably for each configuration sample.

APPENDIX B: DERIVE INTEGRAL FORMULA BY TAKING LIMIT OF THE INCREMENTAL ALGORITHM

The same formula (2) can also be derived by taking a small polynomial power limit of the incremental algorithm [22–24]. Below, we will illustrate those steps. In the incremental algorithm, $S_A^{(2)}$ is computed as

$$\begin{aligned} S_A^{(2)} &= -\sum_{i=1}^{N_k} \ln\left(\frac{\lambda_i}{\lambda_{i-1}}\right), \\ \frac{\lambda_i}{\lambda_{i-1}} &= \frac{\sum P_{s_1} P_{s_2} \mathrm{Tr}\left(\rho_{A;s_1}\rho_{A;s_2}\right)^{(i-1)/N_k} \mathrm{Tr}\left(\rho_{A;s_1}\rho_{A;s_2}\right)^{1/N_k}}{\sum P_{s_1} P_{s_2} \mathrm{Tr}\left(\rho_{A;s_1}\rho_{A;s_2}\right)^{(i-1)/N_k}} \\ &\equiv \langle \mathrm{Tr}\left(\rho_{A;s_1}\rho_{A;s_2}\right)^{1/N_k}\rangle_i. \end{aligned} \tag{B1}$$

The computation for each piece, $-\ln[\langle \mathrm{Tr}(\rho_{A;s_1}\rho_{A;s_2})^{1/N_k}\rangle_i]$, can be computed in parallel and adding them together will derive the final result in Ref. [23]. We notice that the distribution x^{1/N_k} for random variable $x > 0$ will approach a uniform distribution when taking $N_k \to \infty$. Using Jensen's inequality, we take the equality case when we set the $N_k \to \infty$ limit as

$$\begin{aligned} S_A^{(2)} &= -\sum_{i=1}^{N_k} \ln\left[\left\langle \mathrm{Tr}\left(\rho_{A;s_1}\rho_{A;s_2}\right)^{1/N_k}\right\rangle_i\right] \\ &\leqslant -\frac{1}{N_k}\sum_{i=1}^{N_k} \langle \ln\left[\mathrm{Tr}\left(\rho_{A;s_1}\rho_{A;s_2}\right)\right]\rangle_i \\ &\to -\int_0^1 dt \frac{\sum P_{s_1} P_{s_2} \mathrm{Tr}\left(\rho_{A;s_1}\rho_{A;s_2}\right)^t \ln\left[\mathrm{Tr}\left(\rho_{A;s_1}\rho_{A;s_2}\right)\right]}{\sum P_{s_1} P_{s_2} \mathrm{Tr}\left(\rho_{A;s_1}\rho_{A;s_2}\right)^t} \\ &\equiv -\left\langle \ln\left[\mathrm{Tr}\left(\rho_{A;s_1}\rho_{A;s_2}\right)\right]\right\rangle_{s_1,s_2;t}. \end{aligned} \tag{B2}$$

Since we take the $N_k \to \infty$ limit for the integral, $S_A^{(2)} = -\langle \ln[\mathrm{Tr}(\rho_{A;s_1}\rho_{A;s_2})]\rangle_{s_1,s_2;t}$ is exact. Here, our observable becomes $\ln[\mathrm{Tr}(\rho_{A;s_1}\rho_{A;s_2})]$, which is not exponentially small and the integral over continuous field $t \in [0, 1]$ can be realized by numerical integral. This just gives the same formula as Eq. (3)

APPENDIX C: PROVE HUBBARD MODEL IS SIGN PROBLEM FREE

We would like to prove there is no sign problem when computing the exponential observables in the Hubbard model. Because of the well-known particle-hole transformation in the density decoupling channel for bipartite lattices, we define $\tilde{c}^\dagger_{i;\downarrow} \equiv (-1)^i c_{i;\downarrow}$ and have $(I + \tilde{B}_\downarrow)^{-1}_{i,j} = (I + B^*_\uparrow)^{-1}_{i,j}$ so that the weight $P_s \equiv \det(I + B_\uparrow)\det(I + B_\downarrow)$ is always non-negative. This directly indicates that the simulation for free energy should be sign problem free, since the weight there is just P_s^t. As for the proof for the nth Rényi EE, we need to prove that the determinant of the Grover matrix is non-negative for any auxiliary field configuration. First we need a relation $(-1)^{i+j}(I - G_{j,i;\downarrow}) = \tilde{G}_{i,j;\downarrow} \equiv (I + \tilde{B}_\downarrow)^{-1}_{i,j} = (I + B^*_\uparrow)^{-1}_{i,j} = G^*_{i,j;\uparrow} = G^*_{i,j;\downarrow}$, so that $U_c^{-1}(I - G_\downarrow)U_c = G^\dagger_\downarrow$, where U_c is the constant unitary transformation giving $(-1)^i$ coefficient according to the sublattice label. Then we have

$$\begin{aligned} U_c^{-1} D_{s_i} U_c &= U_c^{-1}\left(G^{-1}_{A;s_i} - I\right)U_c = (D^\dagger_{s_i})^{-1}, \\ U_c^{-1}\left(\prod_i D_{s_i}\right)U_c &= \left[\left(\prod_i D_{s_i}\right)^\dagger\right]^{-1}. \end{aligned} \tag{C1}$$

For convenience, we denote e^{Γ_α} as the eigenvalue for $\prod_i D_{s_i}$ and $e^{\lambda_{\alpha;s_i}}$ as the eigenvalue for D_{s_i}. According to Eq. (C1), we have $e^{-\Gamma^*_\alpha} = e^{\Gamma_\beta}$ and $e^{-\lambda^*_{\alpha;s_i}} = e^{\lambda_{\beta;s_i}}$ where α and β can label the same or different eigenvalues and form an injective function. In addition, we have $\det(\prod_i D_{s_i}) = e^{\sum_\alpha \Gamma_\alpha} = e^{\sum_{i,\alpha_i} \lambda_{\alpha_i;s_i}}$. Now we are ready to compute the determinant of the Grover matrix, which is $\det(g_{A,s_1,\ldots,s_n}) = \prod_i \det[(I + D_{s_i})^{-1}]\det(I + \prod_i D_{s_i})$, according to Eq. (C2),

$$g_{A;s_1,s_2,\ldots,s_n} \equiv \prod_i \left(G_{A;s_i}\right)\left[I + \prod_j \left(G^{-1}_{A;s_j} - I\right)\right]. \tag{C2}$$

There aremany summation terms after writing in the $\prod_i D_{s_i}$ and D_{s_i} diagonal basis (i.e., $\det(g_{A,s_1,\ldots,s_n}) = \sum_M \frac{e^{\sum_{\alpha\in M}\Gamma_\alpha}}{\sum_{m_i} e^{\sum_{i,\alpha_i\in m_i}\lambda_{\alpha_i;s_i}}}$, where M and m_i label all the possible choices of choosing eigenvalue sets from $\{\Gamma\}$ and $\{\lambda_{s_i}\}$). For any term written as $\frac{e^{\sum_{\alpha\in M}\Gamma_\alpha}}{\sum_{m_i} e^{\sum_{i,\alpha_i\in m_i}\lambda_{\alpha_i;s_i}}}$, the complex conjugate of it is also in this summation, i.e., $(\frac{e^{\sum_{\alpha\in M}\Gamma_\alpha}}{\sum_{m_i} e^{\sum_{i,\alpha_i\in m_i}\lambda_{\alpha_i;s_i}}})^* = \frac{e^{\sum_{\alpha\notin M'}\Gamma_\alpha}}{\sum_{m_i} e^{\sum_{i,\alpha_i\notin m'_i}\lambda_{\alpha_i;s_i}}}$, where M', m'_i are the mapped eigenvalue set from M, m_i. Since the maps from M, m_i to M', m'_i are injective, for any given M and term in the summation, one can always find one and only one which is the complex conjugate of it so that $\det(g_{A,s_1,\ldots,s_n})$ is always real for one spin sector and non-negative after the square.

[1] J. L. Cardy and I. Peschel, Nucl. Phys. B **300**, 377 (1988).
[2] M. Srednicki, Phys. Rev. Lett. **71**, 666 (1993).
[3] A. Solfanelli, S. Ruffo, S. Succi, and N. Defenu, J. High Energy Phys. 05 (2023) 066.
[4] P. Calabrese and J. Cardy, J. Stat. Mech.: Theory Expt. (2004) P06002.
[5] E. Fradkin and J. E. Moore, Phys. Rev. Lett. **97**, 050404 (2006).
[6] H. Casini and M. Huerta, Nucl. Phys. B **764**, 183 (2007).
[7] T. Grover, Phys. Rev. Lett. **111**, 130402 (2013).
[8] D. Gioev and I. Klich, Phys. Rev. Lett. **96**, 100503 (2006).
[9] B. Swingle, Phys. Rev. Lett. **105**, 050502 (2010).
[10] H. Leschke, A. V. Sobolev, and W. Spitzer, Phys. Rev. Lett. **112**, 160403 (2014).
[11] N. Laflorencie, Phys. Rep. **646**, 1 (2016).
[12] F. F. Assaad, T. C. Lang, and F. Parisen Toldin, Phys. Rev. B **89**, 125121 (2014).
[13] P. Broecker and S. Trebst, J. Stat. Mech.: Theory Expt. (2014) P08015.
[14] P. Broecker and S. Trebst, Phys. Rev. B **94**, 075144 (2016).
[15] P. Broecker and S. Trebst, Phys. Rev. E **94**, 063306 (2016).
[16] V. Alba, Phys. Rev. E **95**, 062132 (2017).
[17] J. D'Emidio, Phys. Rev. Lett. **124**, 110602 (2020).

[18] J. Zhao, Y.-C. Wang, Z. Yan, M. Cheng, and Z. Y. Meng, Phys. Rev. Lett. **128**, 010601 (2022).

[19] J. Zhao, B.-B. Chen, Y.-C. Wang, Z. Yan, M. Cheng, and Z. Y. Meng, npj Quantum Mater. **7**, 69 (2022).

[20] J. D'Emidio, R. Orús, N. Laflorencie, and F. de Juan, Phys. Rev. Lett. **132**, 076502 (2024).

[21] B.-B. Chen, H.-H. Tu, Z. Y. Meng, and M. Cheng, Phys. Rev. B **106**, 094415 (2022).

[22] G. Pan, Y. D. Liao, W. Jiang, J. D'Emidio, Y. Qi, and Z. Y. Meng, Phys. Rev. B **108**, L081123 (2023).

[23] Y. Da Liao, arXiv:2307.10602.

[24] Y. Da Liao, G. Pan, W. Jiang, Y. Qi, and Z. Y. Meng, arXiv:2302.11742.

[25] A. Kitaev and J. Preskill, Phys. Rev. Lett. **96**, 110404 (2006).

[26] M. Levin and X.-G. Wen, Phys. Rev. Lett. **96**, 110405 (2006).

[27] W. Jiang, B.-B. Chen, Z. H. Liu, J. Rong, F. F. Assaad, M. Cheng, K. Sun, and Z. Y. Meng, SciPost Phys. **15**, 082 (2023).

[28] Z. H. Liu, W. Jiang, B.-B. Chen, J. Rong, M. Cheng, K. Sun, Z. Y. Meng, and F. F. Assaad, Phys. Rev. Lett. **130**, 266501 (2023).

[29] M. Song, J. Zhao, M. Cheng, C. Xu, M. M. Scherer, L. Janssen, and Z. Y. Meng, arXiv:2307.02547.

[30] M. Song, T.-T. Wang, and Z. Y. Meng, arXiv:2310.01490.

[31] Z. H. Liu, Y. Da Liao, G. Pan, M. Song, J. Zhao, W. Jiang, C.-M. Jian, Y.-Z. You, F. F. Assaad, Z. Y. Meng, and C. Xu, Phys. Rev. Lett. **132**, 156503 (2024).

[32] X. Zhou, Z. Y. Meng, Y. Qi, and Y. Da Liao, Phys. Rev. B **109**, 165106 (2024).

[33] Y. Da Liao, M. Song, J. Zhao, and Z. Y. Meng, arXiv:2404.13876.

[34] L. Onsager, Phys. Rev. **65**, 117 (1944).

[35] T. D. Schultz, D. C. Mattis, and E. H. Lieb, Rev. Mod. Phys. **36**, 856 (1964).

[36] J. Shao, E.-A. Kim, F. D. M. Haldane, and E. H. Rezayi, Phys. Rev. Lett. **114**, 206402 (2015).

[37] R. V. Mishmash and O. I. Motrunich, Phys. Rev. B **94**, 081110(R) (2016).

[38] E. Y. Loh, J. E. Gubernatis, R. T. Scalettar, S. R. White, D. J. Scalapino, and R. L. Sugar, Phys. Rev. B **41**, 9301 (1990).

[39] G. Pan and Z. Y. Meng, in *Encyclopedia of Condensed Matter Physics*, 2nd ed., edited by T. Chakraborty (Academic Press, Oxford, 2024), pp. 879–893.

[40] X. Zhang, G. Pan, X. Y. Xu, and Z. Y. Meng, Phys. Rev. B **106**, 035121 (2022).

[41] X. Zhang, G. Pan, B.-B. Chen, H. Li, K. Sun, and Z. Y. Meng, Phys. Rev. B **107**, L241105 (2023).

[42] R. Mondaini, S. Tarat, and R. T. Scalettar, Phys. Rev. B **107**, 245144 (2023).

[43] Y. Mou, R. Mondaini, and R. T. Scalettar, Phys. Rev. B **106**, 125116 (2022).

[44] R. Mondaini, S. Tarat, and R. T. Scalettar, Science **375**, 418 (2022).

[45] S. Tarat, B. Xiao, R. Mondaini, and R. T. Scalettar, Phys. Rev. B **105**, 045107 (2022).

[46] N. Ma, J.-S. Sun, G. Pan, C. Cheng, and Z. Yan, arXiv:2301.12438.

[47] J. E. Drut and W. J. Porter, Phys. Rev. B **92**, 125126 (2015).

[48] J. E. Drut and W. J. Porter, Phys. Rev. E **93**, 043301 (2016).

[49] K. Hukushima, Phys. Rev. E **60**, 3606 (1999).

[50] K. Hukushima and K. Nemoto, J. Phys. Soc. Jpn. **65**, 1604 (1996).

[51] F. Assaad and H. Evertz, World-line and determinantal quantum Monte Carlo methods for spins, phonons and electrons, in *Computational Many-Particle Physics*, edited by H. Fehske, R. Schneider, and A. Weiße (Springer, Berlin, 2008), pp. 277–356.

[52] Z.-X. Li, Y.-F. Jiang, and H. Yao, Phys. Rev. B **91**, 241117(R) (2015).

[53] Z. C. Wei, C. Wu, Y. Li, S. Zhang, and T. Xiang, Phys. Rev. Lett. **116**, 250601 (2016).

[54] L. Wang, P. Corboz, and M. Troyer, New J. Phys. **16**, 103008 (2014).

[55] T.-T. Wang and Z. Y. Meng, Phys. Rev. B **108**, L121112 (2023).

[56] R. S. Erramilli, L. V. Iliesiu, P. Kravchuk, A. Liu, D. Poland, and D. Simmons-Duffin, J. High Energy Phys. 02 (2023) 036.

[57] X. Zhang, G. Pan, Y. Zhang, J. Kang, and Z. Y. Meng, Chin. Phys. Lett. **38**, 077305 (2021).

[58] X. Zhang, K. Sun, H. Li, G. Pan, and Z. Y. Meng, Phys. Rev. B **106**, 184517 (2022).

[59] G. Pan, X. Zhang, H. Lu, H. Li, B.-B. Chen, K. Sun, and Z. Y. Meng, Phys. Rev. Lett. **130**, 016401 (2023).

[60] C. Huang, X. Zhang, G. Pan, H. Li, K. Sun, X. Dai, and Z. Y. Meng, Phys. Rev. B **109**, 125404 (2024).

[61] F.-H. Wang and X. Y. Xu, arXiv:2312.14155.

[62] T.-T. Wang, M. Song, L. Lyu, W. Witczak-Krempa, and Z. Y. Meng, arXiv:2402.14916.

[63] Z. Yan and Z. Y. Meng, Nat. Commun. **14**, 2360 (2023).

[64] B.-B. Mao, Y.-M. Ding, and Z. Yan, arXiv:2310.16709.

[65] https://cloud.paratera.com.